

# An Approach for Autonomous Recalibration of Fingerprinting-based Indoor Localization Systems

Ngewi Fet, Marcus Handte, Pedro José Marrón  
Networked Embedded Systems, University of Duisburg-Essen, Germany  
firstname.lastname@uni-due.de

**Abstract**—Fingerprinting-based indoor localization systems tend to achieve higher accuracy compared to other approaches such as signal propagation modeling. However, they also tend to have a higher effort/cost for deployment and maintenance. Changes in the configuration of the indoor space like moving of furniture, or defective signal sources can cause the signal characteristics in the environment to change significantly, and thereby render the fingerprint radio map (used for training the system) outdated. This leads to a drop in localization performance of the system over time. In this paper, we propose an approach to using the system infrastructure for periodically detecting changes in the signal characteristics and autonomously recalibrating the fingerprint radio map. We demonstrate that we can reliably detect changes in signal characteristics stemming from the dampening of a signal source (e.g. induced by moving of furniture) and recalibrate the localization system with an accuracy of 83% to 93% of the optimum localization performance achievable through manual system recalibration.

## I. INTRODUCTION

The past decade has seen a marked increase in the research and development of indoor localization systems, most of which rely on the characteristic signal strength for location estimation. Localization typically involves measuring some signal characteristic in an area, and then applying probabilistic or deterministic techniques to match the signal characteristic to a previously known pattern and obtain a location estimate. Several different technologies have been used in developing localization systems [1] such as WLAN, RFID, GSM, Bluetooth and hybrid combinations thereof. WLAN signals are the most commonly used due to their pervasiveness (as they can be found in almost all buildings nowadays), ease of deployment, and mainstream support in widely available consumer electronics hardware. There are two main WLAN signal characteristic estimation techniques used in localization systems - signal propagation modeling or fingerprinting systems. The signal propagation modeling approach seeks to computationally determine the characteristic signal strength of a particular signal at different areas in the building. This approach greatly reduces the effort for manual calibration during deployment of the localization system but has limitations due to dependency on accuracy of the model and the environment/building materials.

The fingerprinting approach relies on actual measurements (scans) of the signal characteristics of the WLAN signal sources at several positions in the building. These measurements, together with the location where they were measured are then saved as tuples to form a fingerprint. The resulting

radio map (i.e. a collection of fingerprints over the whole area) is used during localization as a reference, whereby signal scans from the environment are matched against signals from the radio map. The location of the closest matching fingerprint is determined to be the current location estimate. RADAR [2] is one of the earliest indoor localization systems which utilizes this approach for fingerprinting and it achieves 50th percentile error distance of 2.67m. There have been refinements to the basic fingerprinting approach and pattern matching over the years which have improved its accuracy and reliability [3] [4].

Unfortunately, the layouts of indoor areas are not always static. For example, a signal source may be moved or disappear over time, and furniture can be moved around as well. These changes in the area layout can alter the characteristic RSSI of the different signals in the space and thereby render the radio map (which was created during deployment) outdated. This can lead to a drop in the accuracy of the localization system, as the radio map is no longer an accurate reflection of the signal characteristics in the area. The more changes occur in the area, the more the localization performance drops and eventually the localization system may become unusable. In this paper, we propose an approach for autonomous recalibration of WLAN fingerprinting-based indoor localization systems. The main contributions are the use of off-the-shelf hardware and custom software to create a localization system architecture wherein the localization infrastructure senses and detects permanent changes in the characteristic RSSI of the signal sources. The detected signal changes can then be used to dynamically recalibrate the signal characteristics of affected areas in the radio map. Since our system is software-based, it can be added to new and existing localization systems with relatively low effort/cost.

The rest of this paper is structured as follows. The next section discusses related work in indoor localization with respect to self-recalibrating and infrastructure-based localization systems. Thereafter, we present our proposed approach to autonomous recalibration of the localization system - spontaneous signal change detection and the recalibration algorithm. The subsequent sections discuss our experimental evaluation of the recalibration system and finally conclude with a summary and directions for future research.

## II. RELATED WORK

One of the challenges facing the development of localization systems is the effort for initial calibration of the system and

maintenance of the localization performance characteristics of the system over time. A lot of research has been done into systems which seek to either reduce or eliminate the calibration effort completely.

Signal propagation model-based systems rely on the computational determination of the path loss incurred by a signal as it travels through space. The path loss for WLAN signals typically follows a log-normal distribution [5], and by applying a range of localization algorithms [6], it is possible to estimate location. Other systems seek to reduce the initial calibration effort, like MapGENIE [7] and ARIADNE [8] use a minimal amount of fingerprints and some information about the building to generate a radio map for the area. SEAMLOC [9] seeks to reduce the effort by combining an interpolation algorithm with measurements at fixed points to estimate location. A similar approach is used by PiLoc [10] to estimate absolute location of mobile devices. In addition, some systems such as [11] have sought to optimize the deployment of access points in the area in order to minimize calibration effort while increasing localization performance. However, these approaches are limited by the difficulty in accurately modeling the propagation of WLAN signals in indoor environments. An accurate model requires a high number of variables, or a limitation thereof, which reduces the complexity of the model and consequently, its performance. Furthermore, the simultaneous localization and mapping systems tend to have lower accuracy immediately after deployment and depend on the active usage of the system.

Although there is much work done on reducing initial calibration effort, there is relatively little work focusing on system recalibration. [12] and [13] rely on sniffers which serve as anchors in the environment and the measurements from these sniffers are used to predict the signal characteristics of the environment and therefore compute location estimates. In [14], the authors propose an approach for spontaneous recalibration of an FM-based localization system by lessening the signal degradation through a combination of signal pre-processing and having pre-defined locations in the environment where the position of the mobile device is known. When situated at these anchors, the mobile device can supply measurements which can be used to recalibrate the system. A similar approach is used in [15] to adjust the location estimate for temporal variations in the signal characteristics. KARMA [16] uses fingerprints which are collected by the mobile devices to model changes in the environment, and then improve the location estimate during the online localization phase. It thus relies on the active usage of the system to maintain performance.

Our approach however, uses the access points both as signal sources and receivers to monitor other access points and detect significant changes in the signal characteristics. This infrastructure-based approach allows us flexibility in deployment and better anticipation of usage patterns which could potentially lead to system performance degradation. It also does not depend on the presence of users actively using the system, and can autonomously adapt to significant changes in the signal characteristics over time.

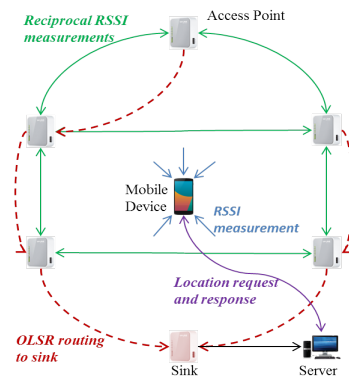


Fig. 1. Overview of system deployment setup

### III. APPROACH

In this section, we present our system architecture and approach to recalibration of the signal characteristics. The basis for our work is a fingerprinting-based localization system which is fully calibrated as is done in most WLAN fingerprinting systems. In order to perform a system recalibration, we need to detect that signal characteristics for an access point have changed, and then use the changes to recalibrate the radio map used for localization. In the following sections, we present in more detail the system architecture, signal change detection and recalibration algorithm for continuous adaptation of the localization system.

#### A. System Setup

Our system infrastructure uses off-the-shelf hardware for the access points. In particular, we use TP-LINK M3020 access points which are small, easily deployable and inexpensive. We install the OpenWRT firmware on the access points and configure two virtual wireless interfaces. One of the interfaces serves as a beacon and actively transmits a WLAN signal, while the other is passive and acts as a sniffer, capturing signal frames from the other access points in the environment. These sniffer measurements from all the deployed access points provide an overview of the state of the signal characteristics in the environment. In order to access these measurements on a continuous basis, we configure one access point to serve as a passive sink for receiving data and configure all the other access points to send their measurements to the sink using the Optimized Link State Routing (OLSR) [17] protocol. Therefore information can flow from one access point to reach any other access point via the resulting wireless mesh network. This eliminates the need for all the access points to have a physical connection to the sink and enables greater flexibility in the deployment of the access points in new or existing localization systems, with better coverage of especially large indoor areas. The sink access point is connected via Ethernet to a server which aggregates the measurements. Figure 1 shows an overview of the resulting system architecture.

After deploying the necessary access points, we calibrate our system by collecting fingerprints of the area with multiple

mobile devices using the method described in [18]. The fingerprints are collected by moving along different paths defined in the building and having the devices continuously scan the area for WLAN signals. The person performing the calibration (trainer) carries multiple devices in both front and back pockets, thereby having them face different orientations so as to mitigate the effects of the presence of the human body during fingerprinting [19]. Several measurements are collected per device along the path walked by the trainer and later aggregated and interpolated along the path to create fingerprints which comprise the signal characteristics and the GPS coordinates of the location. The group of all fingerprints forms the characteristic signal map of the environment which is used for training the localization algorithm. The algorithm used is based on the RADAR algorithm [2], with some additional aggregation for stabilization of temporal effects similar to HORUS [4]. Given a fingerprint scan, the algorithm computes the location probabilities for all fingerprints in the training set and then ranks them from highest to lowest. We then use dynamic deterministic nearest neighbor averaging of the fingerprint matches with the highest probabilities to compute the location estimate. The number of nearest neighbors is set to a minimum value,  $k$ , which expands to include any matching fingerprints with identical probability as the  $k$ -th one.

### B. Signal Change Detection

The deployed access points in our setup each continuously monitor the signal characteristics of the environment and transmit this information to the central server via a sink, as previously described. By examining the aggregated measurements from all access points on the server, it is possible to have an overview of the stability of the system infrastructure for any given time duration. If a significant change occurs in the characteristic RSSI of a particular access point, it will be observed by the other access points in the immediate vicinity. The mesh of co-measurements formed by the access points enables any significant change in one to be immediately measured in multiple links in the network as illustrated in Figure 2. By continuously evaluating these links, it is possible to reliably detect dynamic RSSI changes in the environment. Although WLAN signals are subject to temporal fluctuations [4], for recalibration, we need to determine the access points whose signal characteristics have changed significantly over a measured period of time beyond the threshold of temporal fluctuation. Temporal fluctuations could be caused by people walking past the access points, but we aim to detect sustained changes to the signals which may be due to permanent repositioning of furniture or other items in the environment.

In order to achieve this, we consider two time windows for which we want to determine if there is a change in the signal characteristics. The time windows can be chosen depending on the environment and localization requirements. Given one access point  $A_1$ , we aggregate (by averaging the RSSI per signal source) all the RSSI readings,  $R(A_i)$  collected by  $A_1$  for the two time windows  $t_1$  and  $t_2$ :

$$V_{t1} = \{R_{t1}(A_2), R_{t1}(A_3), \dots, R_{t1}(A_N)\}$$

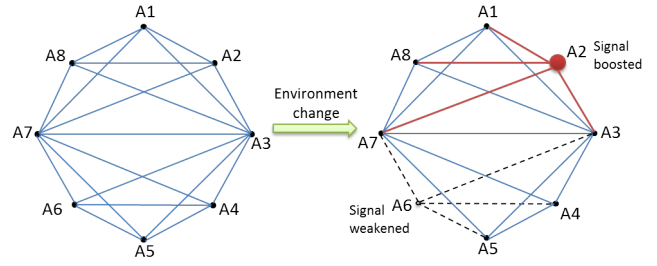


Fig. 2. Link quality change detection in mesh network

$$V_{t2} = \{R_{t2}(A_2), R_{t2}(A_3), \dots, R_{t2}(A_N)\}$$

where  $V$  is the set of aggregated average WLAN RSSI scans and  $N$  is the number of access points in the deployment. We then compute the difference between the average RSSI values between the two time windows for all access points observed by  $A_1$ . Any access points which were not visible in the time range  $t_2$  are assigned a value of -100 dBm which is lower than reported RSSI values and indicates absence of the signal.

$$\delta V = V_{t2} - V_{t1}$$

$$\delta V_{A_1} = ((R_{t2} - R_{t1})_{A_2}, \dots, (R_{t2} - R_{t1})_{A_N})$$

We repeat this process for all access points in the system and thereby generate a list,  $\Delta V$  which is an aggregation of the lists of average RSSI deltas that each access point observes in all other access points between the two time windows:

$$\Delta V = (\delta V_{A_1}, \delta V_{A_2}, \dots, \delta V_{A_N})$$

Given this information, we can now determine those access points whose signal characteristics have significantly changed. Consider again the access point  $A_1$ , we extract the average RSSI delta for  $A_1$ ,  $\delta V_{A_1}$ , from all RSSI delta lists in  $\Delta V$  as follows:

$$M(A_1) = (\delta V_{A_2}(A_1), \delta V_{A_3}(A_1), \dots, \delta V_{A_N}(A_1))$$

$M(A_1)$  only contains measurements from external access points since  $A_1$  cannot measure its own RSSI. We then take the median value of this list of average RSSI deltas for  $A_1$  and compare it against a given threshold for fluctuations. The median metric is analogous to performing a simple majority vote amongst the different observations. If the median,  $\chi_{A_i}$  of all the changes observed is above the threshold for change,  $\tau$ , then the signal characteristics for access point  $A_1$  are considered to have changed significantly.

We repeat this process for all the access points in the system in order to obtain a list of all significantly modified access points where  $\chi_{AP_i} > \tau$ . Previous studies have demonstrated that there is on average temporal fluctuations in the access points of up to 6 dBm [20]. Therefore, we set our change threshold at  $\tau = 8$  dBm in order to clearly differentiate temporal fluctuations from RSSI characteristic changes.

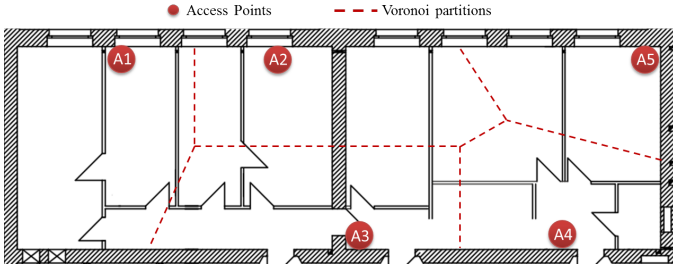


Fig. 3. Building floorplan with access point layout and Voronoi partitions

### C. System Recalibration

Before we use the RSSI delta values observed by the access points for recalibration of the radio map created using the mobile devices, it is necessary to understand how the RSSI measurements from the access points correlate to those from the mobile device. We therefore evaluated the relationship between the access point RSSI measurements and the mobile device RSSI measurements. We collected the RSSI values measured by all the other access points (sniffers) and the mobile devices at fixed increasing distances from each signal source. The correlation of the two data sets matched a linear regression described by:

$$R_r = 1.03 * R_m + 5.78$$

where  $R_r$  and  $R_m$  are the RSSI measured by the access points and mobile devices respectively. The quotient for  $R_m$  is very close to 1 and if we round the constant to the nearest integer (the format in which the RSSI values are reported), then the equation indicates that the access point measurements are on average, approximately 6dBm higher than the mobile device readings. Therefore, when we consider only differences in the RSSI, we can translate RSSI delta observations from the access points to the mobile devices without much loss in accuracy. This approach for using the signal deltas in environments with heterogenous hardware has been shown [21] to improve system stability and localization performance.

For system recalibration, we use the average RSSI delta of the modified access point as observed by each and every other access point in the vicinity. For each access point which observes a change, we apply the delta to all the fingerprints in the radio map which are closest to this access point. The reason being that the fingerprints closest to the access point are most likely to have experienced a similar change as the access point. To this end, we create a Voronoi tessellation of the indoor area with the access points serving as the nodes excluding those access points which have changed significantly. The location coordinates for the access points are dynamically computed from initial calibration radio map using the method described in [22]. The radio map from the initial calibration is thereby grouped into buckets of fingerprints which are closest to a particular access point, each forming a partition as illustrated in Figure 3. During the creation of the Voronoi tessellation, we do not consider any access points whose signal characteristics have been determined to have changed significantly. These

changed access points have potentially skewed observations of all other access points which could be due to some obstacle placed in front of the access point. The observations of the modified access point would therefore not be representative of the signal characteristics in the environment, hence we exclude them during recalibration.

For all the fingerprints in each Voronoi zone, and for each signal scan we add the RSSI delta observed by the anchor node for the corresponding access point. At the end of this process, we would have recalibrated all the fingerprints in the radio map. The generalized recalibration algorithm can be summarized as follows:

```

Input:  $V_{base} = \{R_1(A_1), \dots, R_1(A_N)\}$ 
Input:  $M(A_1) = (\delta V_{A_2}(A_1), \dots, \delta V_{A_N}(A_1))$ 
Output:  $V_{recal} = \{R_2(A_1), \dots, R_2(A_N)\}$ 

detect modified access points
begin
   $C_A$  : set of all changed APs
  foreach  $i \in \{1, \dots, N\}$  do
     $\bar{\chi}_{A_i} : Median(M(A_i))$ 
    if  $\bar{\chi}_{A_i} > \tau$  then
       $C_A \leftarrow A_i$ 
    end
  end
end

compute Voronoi partitions  $P(A_i)$ 
begin
   $P(A_i) = \{P_{A_1}, P_{A_2}, \dots, P_{A_N}\} : A_i \notin C_A$ 
  foreach  $V_j \in V_{base}$  do
     $D_j \leftarrow distance(V_j, A_i) : \forall i = \{1, \dots, N\}$ 
     $D_j$  is minimum  $\Rightarrow P_{A_i} \leftarrow V_j$ 
  end
end

recalibrate fingerprints
begin
  foreach  $A_i \in C_A$  do
    foreach  $V_j \in P(A_i)$  do
       $V_{recal} \leftarrow R_1(A_j) + \delta V_{A_i}(A_j)$ 
    end
  end
end

```

**Algorithm 1:** System recalibration algorithm

We repeat the recalibration process on demand, or on a continuous rolling basis with a fixed period in order to maintain the freshness of the radio map.

## IV. EVALUATION

In this section, we evaluate the performance of our approach to recalibration with respect to the quality of the recalibrated signals and the localization performance over time of the radio map generated through recalibration and the radio map from the initial calibration.

### A. Setup

The experimental evaluation is done in our office area which is 11.5m x 28m in dimension. We set up our localization system as described in our approach in Section III, with 5 access points as depicted in Figure 3. We collect two sets of approximately 2400 fingerprints each in the whole area to form the radio maps for the evaluation of the base system performance. We proceed to dampen the access point  $A_3$  in order to simulate the effects of a change in the signal properties of an access point, and then create two radio maps in this state with approximately 1600 fingerprints each. The access point is dampened by covering it in an aluminium foil sheet in order to have a consistent effect during the course of the evaluation for the different access points. The dampening produces changes in the signal characteristics which are typical of observations we have made when some metal furniture is placed in front of the access point. The same technique is used to successively dampen access points  $A_4$  and  $A_5$ , with radio maps created for each configuration. At the end of the process, we have two radio maps for each of the following configurations:

- B - Base configuration
- D3 -  $A_3$  dampened
- D3\_D4 -  $A_3, A_4$  dampened
- D3\_D4\_D5 -  $A_3, A_4, A_5$  dampened

Furthermore, we perform a recalibration of the signals for each of the dampened configurations. We use the base configuration fingerprints and the signal observations from the different access points as input. The recalibration is performed offline for evaluation purposes, and classified into the following evaluation configurations:

- R3 - Recalibrated after D3
- R3\_R4 - Recalibrated after D3\_D4
- R3\_R4\_R5 - Recalibrated after D3\_D4\_D5

In the next sections, we analyze results of the signal characteristics and localization performance evaluation of the system.

### B. Signal Characteristics

In order to evaluate the effect of the recalibration on the characteristic RSSI of the signals, we compare the signal differences between the different configurations enumerated in evaluation setup. We overlay a grid on the floor plan with 2m x 2m cells and aggregate all the WLAN measurements within each cell to form one characteristic fingerprint reading for the radio maps of each of the configurations. We then compute the differences for each cell between the different configurations. As a starting reference, we compare the measurements between two sets of base, B(1) and B(2). We further compare the RSSI deltas between the B(1) and the D3(1) configuration, as well as the R3 and the D3(1) configuration. Figure 4 shows a visualization of the RSSI differences per cell between the different radio maps overlaid on the floor plan for access point  $A_3$ . The cells where differences in the signal RSSI are observed are colored red, with the intensity of the shade of red being directly proportional to the absolute value of the RSSI delta. To highlight the differences, the

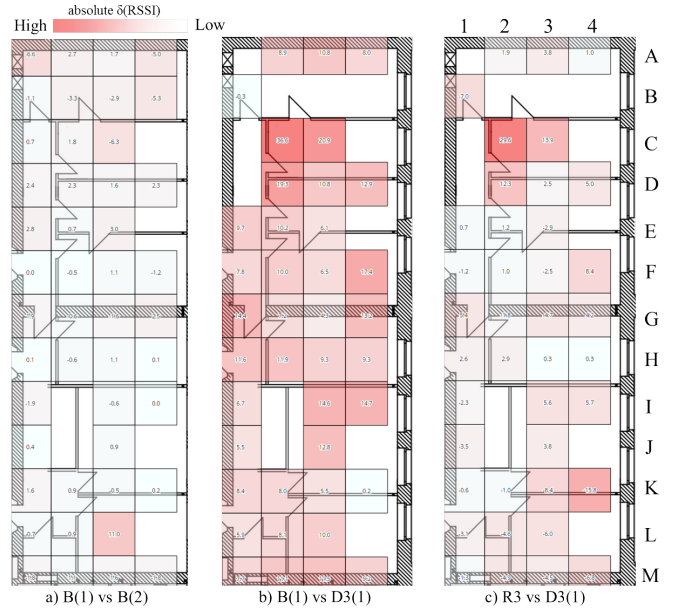


Fig. 4. Signal differences for AP3 in different configurations

visualization only shows the cells where the signal is present in both configurations. We can observe that for the access point  $A_3$ , the two base measurements in Figure 4a are very similar and exhibit only minor temporal RSSI differences, which are generally well within a tolerance of 6 dBm. However, after  $A_3$  is significantly dampened, we observe in Figure 4b that there is a corresponding increase in the RSSI differences between the base radio map and the dampened radio map. There is also a corresponding drop in the occurrences of the signal samples from  $A_3$ . This phenomenon has been observed in previous work [23], that the average number of samples received from a signal drops with reduction in the signal strength. We observe a drop of approximately 70% in the signal occurrences of  $A_3$  between the base radio map and the D3(1) radio map. A similar drop in signal samples was noticeable for the two other dampened configurations as well.

We calculate the signal deltas for  $A_3$  between D3(1) and R3 as depicted in Figure 4c. We can observe that the average RSSI delta drops significantly across the whole area. There are some outliers in cells C2, C3, D2 and K4 which can be attributed to measurement errors in the dampened radio map. Upon further analysis of the RSSI deltas of  $A_3$  in the configurations B(1)-vs-D3(1) and R3-vs-D3(1), we see that they exhibit a strong positive correlation with a Pearson correlation coefficient,  $r_D$  of 0.8.

We repeat the above experiment for all the signal radio map configurations in the evaluation setup and obtain similar results for the other access points  $A_4$  and  $A_5$ . The recalibration of the fingerprint radio map leads to a reduction in the overall average RSSI delta. The results obtained for the different configurations are listed in Table I. We can observe from the data that the average RSSI delta over the whole radio map is very low when comparing two base measured radio maps.

TABLE I  
AVERAGE RSSI DELTA FOR THE COMPARISONS

| AP    | $\delta(\text{B}(1) \text{ vs } \text{B}(2))$ | $\delta(\text{B}(1) \text{ vs } \text{Damp.})$ | $\delta(\text{Rec. vs } \text{Damp.})$ | $r_D$ |
|-------|---|--|--|-------|
| $A_3$ | 1.95  | 10.4   | 4.8                                    | 0.8   |
| $A_4$ | 3.2   | 9.1  | 4.9                                    | 0.8   |
| $A_5$ | 2.2   | 4.3  | 2.4                                    | 0.8   |

where  $\delta$  is the RSSI difference between the configurations (in dBm)  
 $r_D$ : Correlation coefficient of  $\delta(\text{B}(1) \text{ vs } D_i) - \delta(R_i \text{ vs } D_i)$  for access point  $A_i$

However, the average increases dramatically in the dampened radio map and is again reduced after recalibration. The access points  $A_4$  and  $A_5$ , due to their positions in the building, were not visible in all locations of the indoor area and therefore have even less signal samples after dampening. This phenomenon somewhat hides the effect of the dampening, which is more obvious for access point  $A_3$  which is visible in many more locations due to its centralized position in the indoor area.

All three configurations demonstrate a strong positive correlation between the base-vs-dampened RSSI deltas and the recalibrated-vs-dampened RSSI deltas as shown in Table I. This implies that the base and recalibrated radio maps exhibit similar properties with respect to the dampened radio map and are comparable in terms of RSSI characteristics. The recalibration process therefore successfully captures the characteristic RSSI changes in the environment. Thus, by applying the recalibration as described above, we can generate fingerprints that are more representative for the signal propagation in the environment which should improve the accuracy of any fingerprinting-based localization algorithm. In the following section, we quantify this effect for our deployment using one particular algorithm that provides a high accuracy in the base configuration.

### C. Localization Performance

The localization performance evaluation is performed offline on the fingerprints which we created for the different evaluation configurations. The localization algorithm used is described in section III-A, with a deterministic k-nearest neighbor value of 4, determined empirically to achieve the best performance for the base deployment radio maps. In order to get a reference localization accuracy for the evaluation, we compute the accuracy of the localization system using the base configuration radio maps B(1) and B(2) for training and evaluation respectively. We obtain an average error distance of 2.7m, with over 90% of the location matches within 4.4m.

The larger the indoor localization area, the more localized the impact of dampening an access point. The resulting effect of dampening is masked when considering localization performance over the whole indoor area. Therefore during the localization evaluation with dampened configurations, we consider only those fingerprints which contain at least one signal from the affected access point in order to systematically evaluate the actual impact of dampening on the system performance in the local area where the access point is visible. The

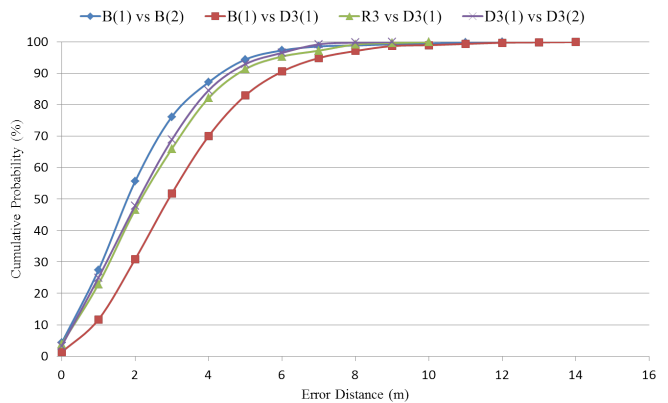


Fig. 5. Localization error distribution for one dampened access point

performance data for localization evaluation taking the whole area into consideration is included in Table II for reference.

We first perform an evaluation with just one access point,  $A_3$  dampened. We use the B(1) radio map as training set and D3(1) as the evaluation set in order to observe the effects of signal dampening on the accuracy. Furthermore, we perform a localization evaluation using R3 as the new training set (after recalibration) and D3(1) as the evaluation set. This gives an indication of the gains in localization performance from periodically recalibrating the B1 training map with the new signal characteristics of the environment. To determine the optimum achievable localization accuracy after dampening, we additionally match our two sets of measurements for D3 against each other. This gives us an indication of the localization performance if we manually recalibrate the system when we detect changes in the signal characteristics of the environment. The system in this state has an average error distance of 2.8m, with 90% of the matches within 4.5m. This indicates that there is a slight drop in the optimum localization performance achievable after one access point is dampened. The cumulative distribution functions of the localization error are illustrated in Figure 5.

We observe that the localization performance of the system drops to an average location error of 3.7m when access point  $A_3$  is dampened, with 90% of the matches within 6m. The error distribution is also lower overall for all the different percentiles of the distribution function. After recalibration is performed, the performance increases again to an average error distance of 3.0m, with 90% of the matches within 5m. This is very close to the optimum achievable localization performance in the D3 configuration, with a difference of only 0.2m of the average error distance compared to manual recalibration. For this experiment, our autonomous recalibration approach is thereby within 93% of the optimum achievable localization performance.

In order to further explore the effect of the dampening and recalibration on the localization system performance, we evaluate the case where there are two dampened access points in the system. This represents the configuration D3\_D4 where the

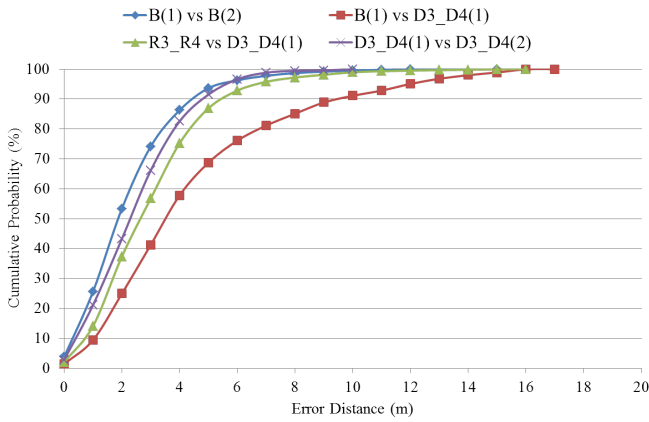


Fig. 6. Localization error distribution for two dampened access points

access points  $A_3$  and  $A_4$  are dampened, and the corresponding recalibrated configuration R3\_R4. Similar to the previous experiment, the optimum achievable localization performance after dampening drops to an average error distance of 3.0m, with 90% of the matches within 5m. We also compare the scenarios of B(1) vs B(2), B(1) vs D3\_D4(1) and R3\_R4 vs D3\_D4(1). We can see from the plot of the cumulative probability distribution function for the error distance in Figure 6, that the impact of dampening two access points is even stronger than for just one, as expected. The average error distance increases from 2.7m for the base performance to 4.9m for the dampened radio map, and then again back down to 3.5m after recalibration. This represents a difference in average error distance of only 0.5m from the optimum performance achievable with manual recalibration of the system. Our approach thereby achieves up to 83.4% of the optimum system performance in this configuration.

TABLE II  
LOCALIZATION AVERAGE ERROR DISTANCE (M)

| Config   | B(1) vs B(2) |       | B(1) vs D(1) |       | R vs D(1) |       | D(1) vs D(2) |       |
|----------|--------------|-------|--------------|-------|-----------|-------|--------------|-------|
|          | All          | $D_s$ | All          | $D_s$ | All       | $D_s$ | All          | $D_s$ |
| D3       | 2.7          | 2.6   | 3.2          | 3.7   | 3.1       | 3.0   | 2.8          | 2.8   |
| D3_D4    | 2.7          | 2.7   | 4.0          | 4.9   | 3.4       | 3.5   | 3.1          | 3.0   |
| D3_D4_D5 | 2.7          | 2.7   | 4.3          | 4.7   | 3.5       | 3.3   | 3.1          | 2.9   |

where  $D_s$ : Localization using only fingerprints with signals from dampened access point in the configuration  $Dx$

We repeat the experiment for the third configuration D3\_D4\_D5 and observe a similar pattern to the previous two discussed cases, as illustrated in Figure 7. Here, our approach achieves an average localization accuracy of up to 86.3% of the optimum achievable localization performance in the dampened state. The average error distance of our approach shows a difference of only 0.4m to the case of a manual recalibration of the system (optimum performance). The localization performance results obtained for the different configuration combinations are summarized in Table II, which includes

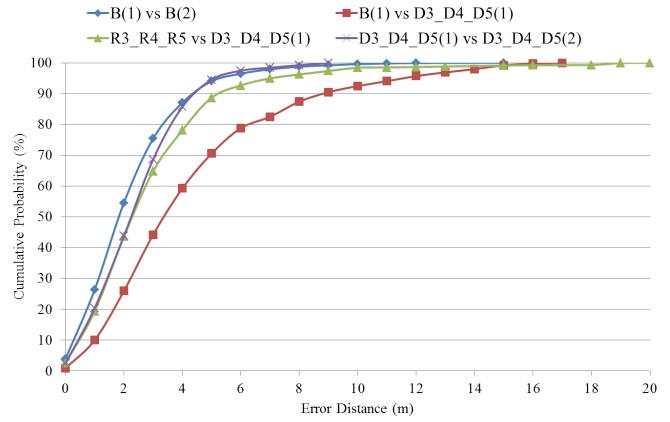


Fig. 7. Localization error distribution for three dampened access points

also the localization performance when all fingerprints in the building were used for localization rather than just those local to the dampened access point signal.

We observe that the average error distance is lower when fingerprints from the whole indoor area are considered than when only fingerprints containing signals from the dampened access points are considered. This is due to the fact that when looking at all fingerprints, the average localization accuracy directly depends on the ratio between the number of affected and unaffected fingerprints. For configurations where only one access point is affected, only measurements in its vicinity (i.e. surrounding the dampened access point) can lead to increased the localization errors. Consequently, when looking at the localization accuracy of the whole area, the impact seems somewhat limited. However, this hides the fact that in the affected area there is a significant performance degradation. By dampening more access points, the affected area (and thus, the fraction of affected fingerprints) increases and as a result, the performance degradation becomes much more noticeable across the whole area.

We take note of the fact that the localization performance for the recalibrated radio map does not quite get back as high the performance of the manually recalibrated radio map. This can be attributed to the fact that the signal propagation path loss (with the accompanying multipath effects) cannot be fully replicated by the recalibration using a constant delta within the different Voronoi partitions. However, the gains from the application of the recalibration are very close to the optimum performance achievable through manual configuration. This means that our recalibration algorithm is able to capture and compensate the most significant impacts on the signal propagation and is therefore worthwhile to apply regularly to a system deployment.

Furthermore, given that the recalibration procedure uses a majority voting to determine which access points have changed, the algorithm becomes inapplicable when more than half of the access points in the deployment experience a sudden change in the signal characteristics. In many practical

cases, this scenario can be avoided by simply increasing the frequency of recalibration of the system which will ensure that any changes to a particular access point are promptly detected and fixed. In other words, our recalibration approach is applicable in areas where there is constant but periodic change in the environment which seriously affects the localization signal. The localization system can be configured to recalibrate the training radio map to match the environmental signal characteristics and thereby significantly limit the decay of the localization performance. In cases where the majority of the access points' signal characteristics do not all change at the same time, the system could detect those that change and recalibrate them.

## V. CONCLUSION

In this paper we have presented an approach to autonomous recalibration of a fingerprint-based indoor localization system. Our approach is software-based using off-the-shelf hardware components, making it cost-effective to deploy in localization systems. Our experimental evaluation results indicate that changes to the signal characteristics induced by dampened signal sources – which can be caused, for example, by moving of furniture – can have a significant negative impact on the localization performance. Our approach can lessen this impact in a fully automated fashion. When quantifying the impact with a specific algorithm that performs well in our deployment, the recalibrated radio map is able to achieve a localization performance of 83% to 93% of the optimum (achievable through manual recalibration). However, since a recalibrated radio map is more representative of the actual signal characteristics, it should lead to performance improvements for any fingerprint-based localization algorithm.

In the future, we plan to extend this work to detect and handle other types of changes which can occur in the environment. Specifically, we are planning to investigate how to detect and handle the movement of access points from one location to another. If such changes can occur in a deployment, we would argue that the infrastructure measurements must be augmented with measurements of mobile devices using the system in order to reliably categorize the change and perform a suitable recalibration.

## ACKNOWLEDGMENT

This work is supported in part by the European Center for Ubiquitous Technologies and Smart Cities (UBICITEC e.V.).

## REFERENCES

- [1] Y. Gu, A. Lo, and I. Niemegeers, "A survey of indoor positioning systems for wireless personal networks," *IEEE Communications Surveys & Tutorials*, vol. 11, no. 1, pp. 13–32, 2009.
- [2] P. Bahl and V. Padmanabhan, "Radar: an in-building rf-based user location and tracking system," in *INFOCOM 2000*, vol. 2. IEEE, 2000, pp. 775–784 vol.2.
- [3] P. Bahl, V. Padmanabhan, and A. Balachandran, "Enhancements to the RADAR user location and tracking system," *Microsoft Research*, vol. 2, no. MSR-TR-2000-12, pp. 775–784, 2000.
- [4] M. Youssef and A. Agrawala, "The Horus location determination system," *Wireless Networks*, vol. 14, no. 3, pp. 357–374, Jan. 2007.
- [5] D. Faria, "Modeling signal attenuation in ieee 802.11 wireless lans-vol. 1," *Computer Science Department, Stanford University*, vol. 1, 2005.
- [6] H. Lee, H. Kim, and W. Choi, "Modeling heterogeneous signal strength characteristics for flexible WLAN indoor localization," *ICCAS-SICE, 2009*, pp. 1765–1768, 2009.
- [7] D. Philipp, P. Baier, C. Dibak, F. Dürr, K. Rothermel, S. Becker, M. Peter, and D. Fritsch, "MapGENIE: Grammar-enhanced indoor map construction from crowd-sourced data," *2014 IEEE International Conference on Pervasive Computing and Communications, PerCom 2014*, pp. 139–147, 2014.
- [8] Y. Ji, S. Biaz, S. Pandey, and P. Agrawal, "ARIADNE," in *Proceedings of the 4th international conference on Mobile systems, applications and services - MobiSys 2006*. New York, New York, USA: ACM Press, 2006, p. 151.
- [9] M. D. Redzic, C. Brennan, and N. E. O'Connor, "SEAMLOC: Seamless indoor localization based on reduced number of calibration points," *IEEE Transactions on Mobile Computing*, vol. 13, no. 6, pp. 1326–1337, 2014.
- [10] C. Luo, H. Hong, and M. C. Chan, "PiLoc: A self-calibrating participatory indoor localization system," in *IPSN-14 Proceedings of the 13th International Symposium on Information Processing in Sensor Networks*. IEEE, Apr. 2014, pp. 143–153.
- [11] M. Ficco, C. Esposito, and A. Napolitano, "Calibrating Indoor Positioning Systems with Low Efforts," *IEEE Transactions on Mobile Computing*, vol. 13, no. 4, pp. 737–751, Apr. 2014.
- [12] S. Gami, A. Krishnakumar, and P. Krishnan, "Infrastructure-based location estimation in WLAN," in *2004 IEEE Wireless Communications and Networking Conference (IEEE Cat. No.04TH8733)*. IEEE, 2004, pp. 465–470.
- [13] P. Krishnan, A. Krishnakumar, C. Mallows, and S. Gamt, "A system for LEASE: location estimation assisted by stationary emitters for indoor RF wireless networks," in *IEEE INFOCOM 2004*, vol. 2. IEEE, 2004, pp. 1001–1011.
- [14] A. Matic, A. Papliatseyeu, V. Osmani, and O. Mayora-Ibarra, "Tuning to your position: FM radio based indoor localization with spontaneous recalibration," in *2010 IEEE International Conference on Pervasive Computing and Communications (PerCom)*. IEEE, Mar. 2010, pp. 153–161.
- [15] Y. Jie, Y. Qiang, and N. Lionel, "Adaptive Temporal Radio Maps for Indoor Location Estimation," *Pervasive Computing and Communications, 2005. PerCom 2005. Third IEEE International Conference on*, no. PerCom, pp. 85–94, 2005.
- [16] P. Sharma, D. Chakraborty, N. Banerjee, D. Banerjee, S. K. Agarwal, and S. Mittal, "KARMA: Improving WiFi-based indoor localization with dynamic causality calibration," in *2014 Eleventh Annual IEEE International Conference on Sensing, Communication, and Networking (SECON)*. IEEE, Jun. 2014, pp. 90–98.
- [17] P. Jacquet, P. Muhlethaler, T. Clausen, A. Laouiti, A. Qayyum, and L. Viennot, "Optimized link state routing protocol for ad hoc networks," in *Multi Topic Conference, 2001. IEEE INMIC 2001. Technology for the 21st Century. Proceedings. IEEE International*, 2001, pp. 62–68.
- [18] N. Fet, M. Handte, S. Wagner, and P. Marrón, "Enhancements to the LOCOSmotion Person Tracking System," in *Evaluating AAL Systems Through Competitive Benchmarking*, ser. Communications in Computer and Information Science, J. Botía, J. Álvarez García, K. Fujinami, P. Barsocchi, and T. Riedel, Eds. Springer Berlin Heidelberg, 2013, vol. 386, pp. 72–82.
- [19] N. Fet, M. Handte, and P. J. Marrón, "A model for WLAN signal attenuation of the human body," in *Proceedings of the 2013 ACM international joint conference on Pervasive and ubiquitous computing - UbiComp '13*. New York, New York, USA: ACM Press, 2013, p. 499.
- [20] K. Kaemarungsi and P. Krishnamurthy, "Properties of indoor received signal strength for WLAN location fingerprinting," *MOBIQUITOUS 2004.*, pp. 14–23, 2004.
- [21] M. B. Kjærsgaard, "Indoor location fingerprinting with heterogeneous clients," *Pervasive and Mobile Computing*, vol. 7, no. 1, pp. 31–43, 2011.
- [22] D. Han, D. G. Andersen, M. Kaminsky, K. Papagiannaki, and S. Seshan, "Access Point Localization Using Local Signal Strength Gradient," in *Passive and Active Network Measurement*, 2009, pp. 99–108.
- [23] M. Youssef, a. Agrawala, and a. Udaya Shankar, "WLAN location determination via clustering and probability distributions," *Proceedings of the First IEEE International Conference on Pervasive Computing and Communications, 2003. (PerCom 2003).*, pp. 143–150, 2003.